

Quadratic transverse anisotropy term due to dislocations in Mn₁₂-Ac crystals directly observed by EPR spectroscopy

R. Amigo, E. del Barco, *Ll. Casas, *E. Molins, and J. Tejada

Departamento de Física Fundamental, Universidad de Barcelona

Diagonal 647, Barcelona, 08028, Spain

**Instituto de Ciencia de Materiales de Barcelona (CSIC). 08193 Cerdanyola. Spain*

I. B. Rutel, **B. Mommouton, N. Dalal, and J. Brooks

NHMFL/FSU, CM/T group 1800 E.P.Dirac dr. Tallahassee, FLORIDA 32310

***Institut National des Sciences Appliquées. Toulouse. France*

(11/01/01)

Abstract

High-Sensitivity Electron Paramagnetic Resonance experiments have been carried out in fresh and stressed Mn₁₂-Acetate single crystals for frequencies ranging from 40 GHz up to 110 GHz. The high number of crystal dislocations formed in the stressing process introduces a $E(S_x^2 - S_y^2)$ transverse anisotropy term in the spin hamiltonian. From the behaviour of the resonant absorptions on the applied transverse magnetic field we have obtained an average value for $E = 22$ mK, corresponding to a concentration of dislocations per unit cell of $c = 10^{-3}$.

Since J. Friedman et al. found the stepwise magnetic hysteresis on Mn_{12} -Acetate molecular cluster, and interpreted it in terms of resonant quantum tunneling [1], a huge number of experimental measurements have been carried out on this compound [2–10](see also references herein), showing its quantum behaviour under many different experimental techniques. Mn_{12} -Ac is a spin 10 molecular cluster which forms macroscopic single crystals in which all the molecules are identical and they take the same spacial orientation respect to the crystallographic axes. The magnetic structure of the spin $S = 10$ of each molecule is represented, in first approximation, by the Hamiltonian $H = -DS_z^2 - g\mu_B\mathbf{S} \cdot \mathbf{H}$, where D is the uniaxial anisotropy constant, g is the Lande factor, μ_B is the Bohr magneton and \mathbf{H} is the applied magnetic field. In the absence of external field, opposite sign levels of the $2S+1$ S_z components of the spin S are degenerated in energy two to two in the both sides of the anisotropy barrier $U = DS^2$. When a longitudinal magnetic field, H_z , is applied, the spin levels in the direction of the field become more stable and the system relaxes towards the new equilibrium state. It has been firmly established experimentally that this relaxation can occur via quantum tunneling. However, in the absence of transverse components of external magnetic fields, the uniaxial Hamiltonian cannot explain the quantum relaxation. Hamiltonian terms not commuting with S_z are needed in order to explain the observed quantum phenomena. Due to the tetragonal symmetry of the Mn_{12} -Ac crystals, transverse anisotropy terms which are quadratic on the spin operator are not allowed. The lowest order transverse terms are those proportional to $S_+^4 + S_-^4$ [11], otherwise, these terms imply that quantum tunneling can not occur at all the resonant fields, $H_z = nD$, contrary to the experimental observations in Mn_{12} -Ac. To explain the presence of quantum tunneling at any resonant field there have been several theoretical approaches, including the transverse component of the magnetic field due to dipolar intermolecule interactions or hyperfine interaction with the nuclei spin of the manganese atoms [12–17]. However, from the magnetic relaxation experiments [1–4,8–10], it seems to be necessary stronger magnetic fields than dipolar or hyperfine fields in order to explain the high value of the quantum relaxation that Mn_{12} -Ac exhibits. Recently, Chudnovsky and Garanin [18,19] have suggested a new theoretical approach which

explains the quantum behaviour of $\text{Mn}_{12}\text{-Ac}$ in terms of dislocations existing in the crystals. They propose that crystal dislocations introduce quadratic terms on S_x and S_y , producing tunneling in a lower order of perturbation theory than the transverse-field. Unpublished experimental results seem to support this new theory [20–23]. In this paper we will show a new experimental approach which indicates that dislocations formed in a strongly stressed single crystal introduce the $E(S_x^2 - S_y^2)$ term suggested by Chudnovsky and Garanin, where E is the transverse anisotropy constant.

The $\text{Mn}_{12}\text{-Ac}$ organometallic cluster forms a molecular crystal of tetragonal symmetry with the lattice parameters $a = 1.732$ nm and $c = 1.239$ nm [24]. The unit cell contains two $\text{Mn}_{12}\text{O}_{12}$ molecules surrounded by four water molecules and two acetic acid molecules. In the crystallization process point defects usually appear in a low number along the whole crystal. It has been shown experimentally that dislocations can be created in a $\text{Mn}_{12}\text{-Ac}$ single crystal by rapid thermal cycles, in which the high change of temperature in a low scale of time produces radial and tangential tensions between the core and the surface of the crystal [21,22]. It is easy to visualize that tensions and pressure forces produced by mechanical distortion of the crystal may generate the same kind of dislocations in a single crystal. This is exactly what we have done with a $\text{Mn}_{12}\text{-Ac}$ single crystal. When a dislocation is created inside the crystal it has produced a disorder of the molecules in the vicinity of the dislocation. As the number of dislocations in the crystal grows the disorder extends over the whole crystal converting it in a mosaic crystal. The mosaicity is related to the number of dislocations existing in the crystal and can be determined experimentally by analyzing the width of the X-ray diffraction peaks [25–27].

In our experiments we have used two single crystals: a) fresh single crystal and b) strongly stressed single crystal. To distort the crystal we put it in a glue by one of the extremities. Then a gradually increasing force was applied to the other extreme, perpendicular to the longer length, until the the crystal fractured. Then, the longer resulting part of the crystal was adequately cleaned and tested by X-ray diffraction to be sure that it was a single crystal. Both samples were characterized by X-ray analysis before making the EPR experiments. To

obtain a fine check of the variation of the mosaicity between fresh and stressed crystals we have used low angle difraction peaks in order to minimize the widening associated to the lack of monochromaticity of the $K_{\alpha 1}$ and $K_{\alpha 2}$ X-ray emission lines of Mo element. We used a four-circle single-crystal X-ray diffractometer (Enraf-Nonius CAD4, MoKa radiation) in the characterisation. Reflections ($\pm 2, \pm 2, \pm 2$) were studied for both fresh and stressed single crystals. Peak intensities of the stressed crystal were normalised according to the measured volume of the studied fragment. Figure 1 shows $\Delta\omega - \Delta(2\theta)$ plot of (2,2,-2) reflection for the fresh (left) and stressed crystal (right). An enlargement of the peak width along the ω direction is clearly observed although there is not a significant change along the 2θ direction (see inset of figure 1). Assuming that the distance between dislocations is inversely related to the widening of the reflection peak in the ω direction [21,25] we can conclude that the stressed crystal has a larger mosaicity than the fresh one. As the ω peak-width in the stressed crystal is a factor about 2 higher than in the fresh crystal, we can conclude that the number of dislocations increases about one order of magnitude in the distortion process.

The high frequency resonance experiments have been carried out using the AB millimeter wave vector network analyzer (MVNA) [28]. The base frequency obtained from this source (range 8 - 18 GHz) is multiplied by Q, V and W Schottkey's diodes to obtain frequency range used in our experiment (37 - 109 GHz). The sample, a single $\text{Mn}_{12}\text{-Ac}$ crystal, is placed on the bottom of the cylindrical resonant cavity, halfway between its axis and perimeter. The applied dc magnetic field is parallel to the cavity axis and approximately perpendicular to the easy (c) axis of the crystal. The experiment frequencies are TE_{0np} ($n, p = 1, 2, 3, \dots$) which are the resonant frequencies for the cavity used. Resonance Q-factor varies from 20000 at TE_{011} mode (41.6 GHz) to a few thousand at higher frequencies. Due to the high sensitivity at resonance, there is an increase over conventional EPR of almost 3 order of magnitude, allowing for the detaction of the absorption peaks suggested theoretically by the diagonalization of the corresponding spin Hamiltonian.

The spin Hamiltonian used to explain the experimental data obtained in the last years is

$$\mathcal{H} = -DS_z^2 - BS_z^4 + C(S_+^4 + S_-^4) - g\mu_B \mathbf{H} \cdot \mathbf{S} \quad (1)$$

where D , B , and C parameters have been experimentally obtained by EPR, Neutron spectroscopy and magnetic relaxation experiments [1–6,9,10,29–32]. \mathbf{H} is the applied magnetic field. The component of the applied magnetic field parallel to the easy axis direction, called longitudinal component, $H_{\parallel} = H \sin \theta$, changes the barrier height between the two classical spin orientations, while the component of the field on the hard plane, transverse component, $H_{\perp} = H \cos \theta$, affects the overlapping of the respective wave functions, which determines the quantum splitting of the degenerate spin states. In the absence of longitudinal field, the quantum splitting of the different m spin levels, Δ_m , and consequently the rate of resonant tunneling between the spin levels depend on the magnitude of the transverse component H_{\perp} . The evolution of the spin levels in the two wells, as a function of the intensity of the transverse component of the field, can be deduced from the diagonalization of the spin Hamiltonian of equation (1). In the transmission spectra of our EPR experiments we can detect absorptions peaks corresponding to the absorption of radiation of frequency f by the transitions effectuated between the spin levels of the Hamiltonian with energy difference equal to hf . From the field position of these peaks we can extract the behaviour of the quantum splittings on the transverse magnetic field. The results obtained with the fresh crystal are plotted in figure 2 (solid circles). The experiments have been done at frequencies ranging from 50 GHz up to 110 GHz and fields up to 9 T, placing the crystal with the easy z -axis perpendicular to the field direction. We have found the best fitting of our data for $D = 555$ mK, $B = 1.3$ mK, and $C = 2.2 \times 10^{-2}$ mK (solid lines in figure 2), in good agreement with the values given in references [6,29,32]. From this figure, it is clearly observed that the dependence of the quantum splittings (Δ_{10} first right line, Δ_9 second, Δ_8 third, and so on) on the transverse field is matching perfectly with the theoretical calculation. The lines that appear at high frequencies and round going down and up with the field correspond to the energy difference between different quantum splittings. However, there are four points appearing at low frequencies between ground splitting and first excited splitting lines which

do not have a conventional explanation. These peaks appear also in the experiments done by Hill et al. [6] and the authors can not give any explanation. The presence of these peaks constitute an incognita for us too.

In figure 3 we show the EPR absorption spectra recorded at $f = 67$ GHz for both fresh (A) and stressed (B) $\text{Mn}_{12}\text{-Ac}$ single crystals. The labelling used in the figure $\alpha_{m,\varphi}$ refers to the Δ_m splitting absorptions with the field applied perpendicular to the easy axis with an angle, φ , with respect to the x magnetic axis. For a fresh crystal, represented by the Hamiltonian (1), there is a symmetry between any direction perpendicular to the easy axis. The peaks observed for fresh crystal correspond to the resonances with the splittings Δ_9 , Δ_8 , Δ_7 , and so on, as has been shown in figure 2. However, for the stressed crystal, each α_m absorption peak appears doubled. This phenomena can be explained by the addition of a $E(S_x^2 - S_y^2)$ term to the Hamiltonian (1), as Chusdovsky and Garanin suggest as an effect of dislocations [18,19]. This term introduces the hardest anisotropy along the x -axis, while y -axis remains as a medium anisotropy axis. For this reason, different directions of the applied field give different values of each quantum splitting, $\Delta_{m,\varphi}$. This is the same behaviour observed in the powder sample of Fe_8 molecular clusters [33–35]. The angular dependence of $\Delta(\varphi)$ at a fixed value of the transverse component of the field is not monotonic. Because of the shape of the function $\Delta(\varphi)$, for a sample with hard axis oriented at random, that is with not preference for any angle φ , there are two values of Δ for which the density of states has a peak. These are the values of the splitting corresponding to $\varphi = 0$ and $\varphi = \frac{\pi}{2}$ (see references [34] and [35]). In the absence of dissipation, the contribution of each Mn_{12} molecule to the imaginary part of the susceptibility is proportional to $\delta(\omega - \frac{\Delta[\varphi, H_\perp]}{\hbar})$. However, the total imaginary part of the susceptibility is,

$$\chi'' \propto \int_0^\pi g(\varphi) \delta(\omega - \frac{\Delta[\varphi, H_\perp]}{\hbar}) d\varphi , \quad (2)$$

where $g(\varphi)$ is the distribution of molecules on φ . For a fresh crystal, having no significant number of dislocations, there is an equivalence between x and y -axes as the Hamiltonian (1) has no preference for any transverse direction. Due to this, the splitting does not depend on

ϕ and the amplitude A of the absorption of electromagnetic radiation must have only one peak corresponding to $\Delta[H_{\perp}] = hf$, as it can be seen in figures 2 and 3A. On the contrary, in a strongly stressed single crystal of Mn_{12} the dislocations are randomly affecting the magnetic structure of the molecular clusters, introducing the term $E(S_x^2 - S_y^2)$ in different manner for each molecule [18,19]. That is, the fact that the effect of the dislocations existing in a single crystal depends on its direction along the crystal and on the distance to a given molecule may be considered as a random generation of a x -hard-axis for each molecule. For this reason, a Mn_{12} -Ac single crystal with a large mosaicity can be approximated as a powder sample with x -axis of the molecules oriented at random. In this case, Eq. (2) can be rewritten as

$$\chi'' \propto \int_0^\infty \delta(\omega - \frac{\Delta[\varphi, H_{\perp}]}{\hbar}) \left(\frac{d\Delta}{d\varphi} \right)^{-1} d\Delta = \left(\frac{d\Delta}{d\varphi} \right)^{-1} \Big|_{\Delta=\hbar\omega}. \quad (3)$$

Therefore, there are two field values, solutions of the equations $\Delta[0, H_{\perp 1}] = hf$ and $\Delta[\frac{\pi}{2}, H_{\perp 2}] = hf$, at which the amplitude of the absorption is maximal. Due to this, the two doubled peaks of each splitting observed in the stressed single crystal (figure 3) can be attributed to the two mean orientations of the splitting Δ on the angle φ , $\Delta_{m,0}$ and $\Delta_{m,\pi/2}$. As the distance between the two doubled peaks basically depends on the parameter E we can extract a first value of $E \sim 20$ mK.

A more precise analysis of the effect of dislocations on the spin Hamiltonian of Mn_{12} -Ac can be achieved by studying the behaviour of the quantum splittings on the transverse magnetic field. Thus, EPR experiments have been done in the stressed crystal for many frequencies ranging from 40 Ghz up to 110 GHz. In figure 4, it has been plotted the field position of the EPR absorption peaks found at the experiment frequencies f (open circles). The EPR data have been fitted by using the magnetic level structure resulting from the diagonalization of the Hamiltonian (1), adding the term $E(S_x^2 - S_y^2)$ attributed to the effect of the dislocations. The results of our fitting procedure are shown in figure 4. Black lines correspond to $\varphi = 0$ and blue lines correspond to $\varphi = \pi/2$. The values of the Hamiltonian parameters used in our fitting procedure are $D = 675$ mK, $B = 0.9$ mK, $C = 1.8 \times 10^{-2}$

mK, and $E = 22$ mK. Comparing these values with the values extracted from the fitting of the fresh crystal absorption peaks of figure 2 one can conclude that dislocations introduce a general variation of the spin Hamiltonian, apart for the introduction of the transverse anisotropy term. This effect of dislocations on the magnetic structure of the molecules on the vicinity is expected in the theoretical model of Chudnovsky and Garanin [18,19]. As the authors observe, dislocations may introduce other effects, for example, transverse magnetic fields. This effect has not been considered in our analysis because its complexity. However, we can extract quantitative information of the number of dislocations existing in the stressed single crystal by analyzing the distribution of the generated transverse anisotropies. From the theoretical model [19], one can extract the distribution of the logarithm of the transverse anisotropy, $\ln(E/2D)$, as a function of the concentration of dislocations per unit cell, c . This distribution function has a maximum at a different value of $E/2D$ depending on c . If we assume that the observed absorption peaks correspond to this maximum in the distribution, we can extract an approximated value of c from the resulting Hamiltonian parameters from the fit of the experimentally obtained radiation spectra. We have obtained $\ln(E/2D) = -4.1$. This corresponds to a concentration of dislocations per unit cell of $c \sim 10^{-3}$, in good agreement with the theoretical estimation [19], and with the experimental results [20–22] for a similar samples. Using the comparison X-ray analysis of the mosaicity for both fresh and stressed crystals of figure 1, one can observe that the number of dislocations is increased by almost one order of magnitude than the fresh sample. We conclude that in a fresh crystal the number of dislocations per unit cell is approximately $c \sim 10^{-4}$.

Through high-sensitivity EPR experiments carried out in a strongly stressed single crystal of $\text{Mn}_{12}\text{-Acetate}$ we have directly obtained the magnitude of the transverse anisotropy term $E(S_x^2 - S_y^2)$, with $E = 22$ mK, associated to dislocations existing in the crystal. We have estimated the value of the concentration of dislocations per unit cell in both fresh and stressed crystals. It may be also possible that the the combined effect of a heavy X-ray irradiation dose and subsequent thermal stressing treatment create a large number of new defective sites and extends the original ones. These sites will necessarily have a lower symmetry and

could lead to new EPR absorption peaks, with an *E*-term, such as determined here. A clear effect of lattice defects on magnetization tunneling has been detected recently [20–22]. We also note that an EPR line-broadening effect of naturally present defects in Mn₁₂ and Fe₈ single crystals has been reported recently [36]. Additional investigations are thus needed in order to clearly understand the origin of the newly found EPR peaks in the present work.

This work was supported by MEC Grant number PB-96-0169 and EC Grant number IST-1929. Work at NHMFL/FSU was supported through a contractual agreement between the NSF through Grant No. NSF-DMR-95-27035 and the State of Florida.

FIGURE CAPTIONS

Figure 1: $\Delta\omega$ - $\Delta(2\theta)$ plot of both fresh (left) and stressed (right) $\text{Mn}_{12}\text{-Ac}$ single crystals for (2,2,-2) reflection. Increase of imperfections is evidenced by broadening along ω direction.

Figure 2: Resonant peaks from fresh single crystal of $\text{Mn}_{12}\text{-Ac}$ for different frequencies, ranging from 50 GHz up to 110 GHz, as a function of the magnetic field applied perpendicularly to the magnetic easy axis direction of the crystal. The solid lines are the fitting result of the diagonalization of the spin Hamiltonian of eq. (1).

Figure 3: EPR spectra recorded at 67 GHz for both fresh (A) and stressed (B) single crystals of $\text{Mn}_{12}\text{-Ac}$. The experiments were done at $T = 10$ K. The peaks are associated to the different quantum splittings through the next nomenclature: $\Delta_{m,\varphi}$.

Figure 4: EPR peaks for the stressed single crystal of $\text{Mn}_{12}\text{-Ac}$. The data are fitted by adding the term $E(S_x^2 - S_y^2)$ to the Hamiltonian of eq. (1). The fitting lines represent the field behaviour of the quantum splittings for $\varphi = 0$ (black lines) and $\varphi = \pi/2$ (blue lines).

REFERENCES

- [1] J. R. Friedman, M. P. Sarachik, J. Tejada, and R. Ziolo, Phys. Rev. Lett. **76**, 3830 (1996)
- [2] J. M. Hernandez, X. X. Zhang, F. Luis, J. Bartolome, J. Tejada and R. F. Ziolo, Europhys. Lett. **35**, 301 (1996).
- [3] L. Thomas, F. Lioni, R. Ballou, D. Gatteschi, R. Sessoli, and B. Barbara, Nature **383**, 145 (1996).
- [4] F. Luis, J. M. Hernandez, J. Bartolome, and J. Tejada, Nanotechnology, **10**, 86 (1999).
- [5] J. A. A. Perenboom, J. S. Brooks, S. Hill, T. Hathaway, and N. Dalal, Phys. Rev. B**58**, 330 (1998).
- [6] S. Hill, J. A. A. Perenboom, N. S. Dalal, T. Hathaway, T. Stalcup, and J.S. Brooks, Phys. Rev. Lett. **80**, 2453 (1998).
- [7] A. Fort, A. Rettori, J. Villain, D. Gatteschi, and R. Sessoli, Phys. Rev. Lett. **80**, 612 (1998).
- [8] W. Wernsdorfer, R. Sessoli, and D. Gatteschi, Europhys. Lett. **47**, 254 (1999).
- [9] L. Bokacheva, A. D. Kent, and M. A. Walters, Phys. Rev. Lett. **85**, 4803 (2000).
- [10] A. D. Kent, Y. Zhong, L. Bokacheva, D. Ruiz, D. N. Hendrikson, and M. P. Sarachik, Europhys. Lett. **49**, 521 (2000).
- [11] F. Hartmann-Boutron, P. Politi, and J. Villain, Int. J. Mod. Phys. B**10**, 2577 (1996).
- [12] N. V. Prokof'ev, and P. C. E. Stamp, Phys. Rev. Lett. **80**, 5794 (1998).
- [13] D. A. Garanin, E. M. Chudnovsky, and R. Schilling, Phys. Rev. B**61**, 12204 (2000).
- [14] E. M. Chudnovsky, Phys. Rev. Lett. **84**, 5676 (2000).
- [15] N. V. Prokof'ev, and P. C. E. Stamp, Phys. Rev. Lett. **84**, 5677 (2000).

- [16] W. Wernsdorfer, C. Paulsen, and R. Sessoli, Phys. Rev. Lett. **84**, 5678 (2000).
- [17] S. Miyashita, and K. Saito, ArXiv:cond-mat/0005013.
- [18] E. M. Chudnovsky, and D. A. Garanin, arXiv:cond-mat/0105195.
- [19] D. A. Garanin, and E. M. Chudnovsky, arXiv:cond-mat/0105518.
- [20] K. M. Mertes et al., arXiv:cond-mat/0106579.
- [21] J. M. Hernandez, F. Torres, J. Tejada, and E. Molins, arXiv:cond-mat/0110515.
- [22] F. Torres, J. M. Hernandez, E. Molins and J. Tejada, arXiv:cond-mat/0110538.
- [23] The combination of both X-ray irradiation and mechanical stressing may be additive in the process of dislocations and defects creation.
- [24] T. Lis, Acta Crystallogr. B**36**, 4024 (1980).
- [25] R. I. Barabash, *X-ray Analysis of precipitation-related crystals with dislocation substructure*. Pages 127-140 in *Defect and Microstructure analysis by diffraction*, by R. L. Snyder, J. Fiala, and H. J. Bunge. IUCr Monographs on Crystallography 10. Oxford University Press (1999).
- [26] A. McL. Mathieson, Acta Cryst. A**38**, 378 (1982).
- [27] A. McL. Mathieson, and A. W. Stevenson, Acta Cryst. A**41**, 223 (1986).
- [28] Manufactured by Abmm, 52 Rue Lhomond, 75005 Paris, France.
- [29] A. L. Barra, D. Gatteschi, and R. Sessoli, Phys. Rev. B**56**, 8192 (1997).
- [30] A. Mukhin, V. D. Travkin, A. K. Zvezdin, S. P. Lebedev, A. Caneschi and D. Gatteschi, Europhys. Lett. **44**, 778 (1998).
- [31] Y. Zhong et al., J. Appl. Phys. **85**, 5636 (1999).
- [32] I. Mirebeau, M. Henion, H. Casalta, H. Andres, H. U. Gdel, A. V. Irodova, and A.

Caneshi, Phys. Rev. Lett. **83**, 628 (1999).

[33] W. Wernsdorfer and R. Sessoli. Science **284**, 133 (1999).

[34] E. del Barco, N. Vernier, J. M. Hernandez, J. Tejada, E. M. Chudnovsky, E. Molins, and G. Bellesa, Europhys. Lett, **47**, 722-728 (1999).

[35] E. del Barco, J. M. Hernandez, J. Tejada, N. Biskup, R. Achey, I. Rutel, N. Dalal, and J. Brooks, Phys. Rev. B**62**, 3018 (2000).

[36] Kyungwha Park, M. Novotny, N. S. Dalal, S. Hill, and P. Rikvold, Phys. Rev. B, (in press); arXiv:cond-mat/0106276.

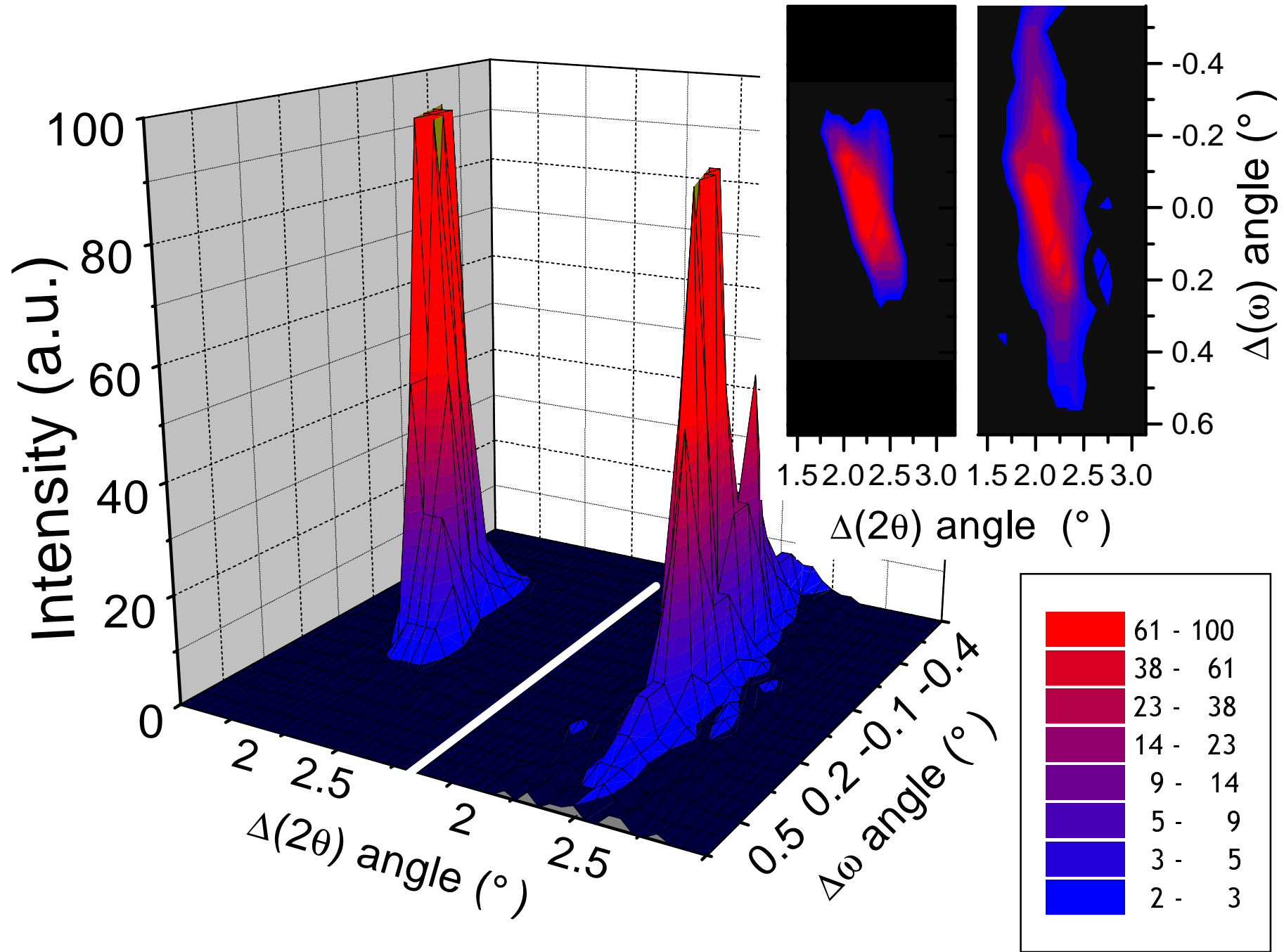


Figure 1: Amigo et al.

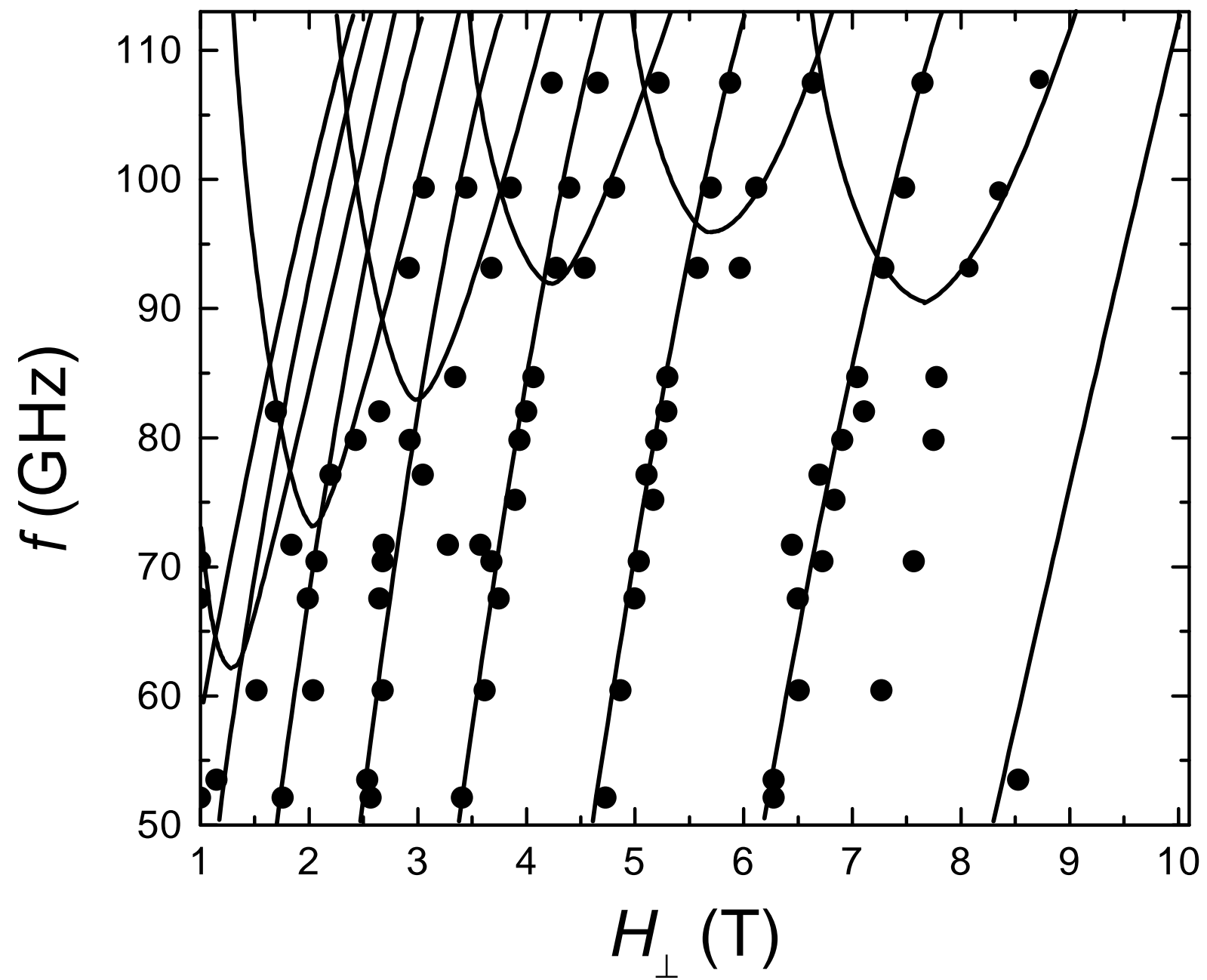


Figure 2: Amigo et al.

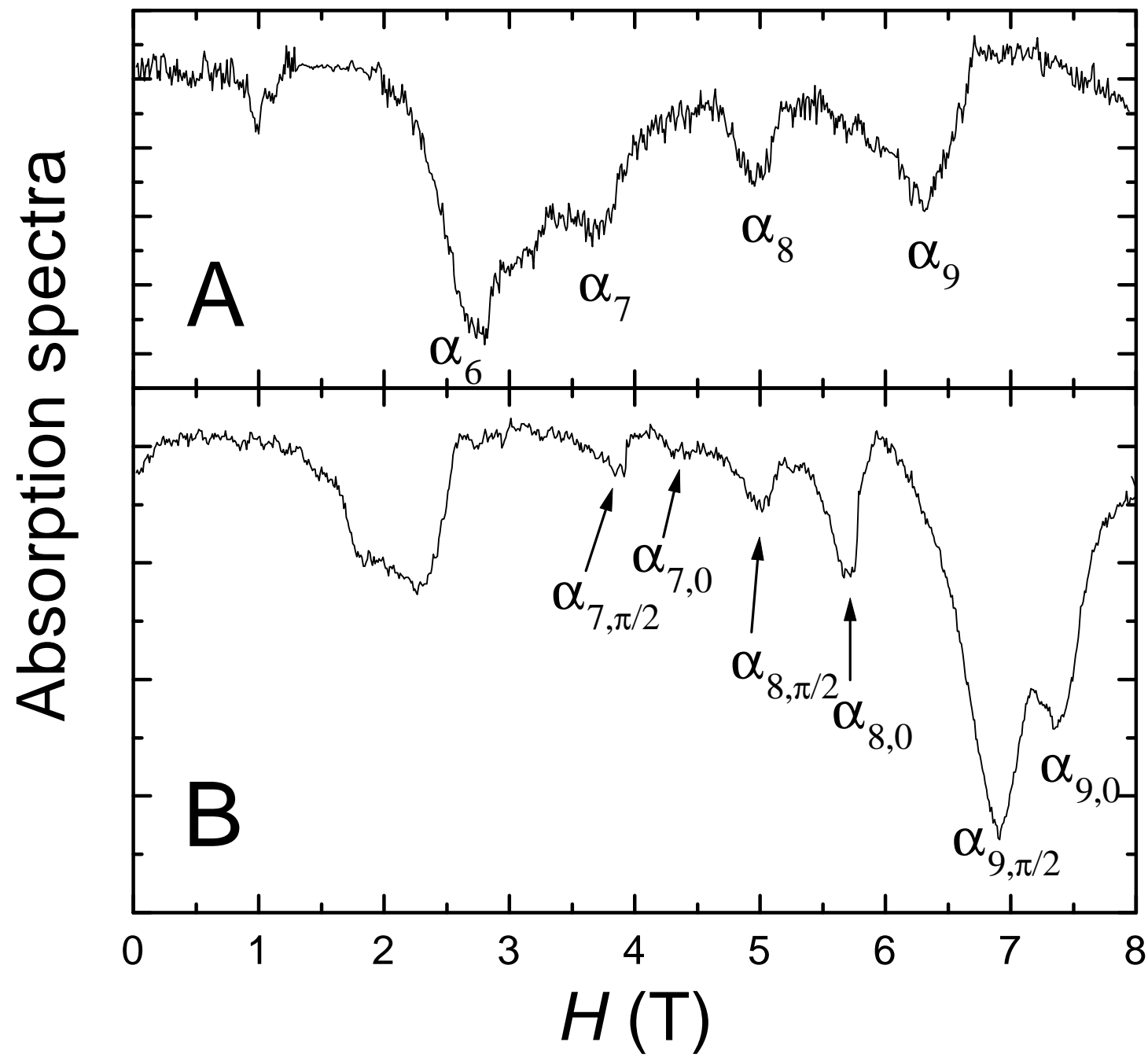


Figure 3: R. Amigo et al.

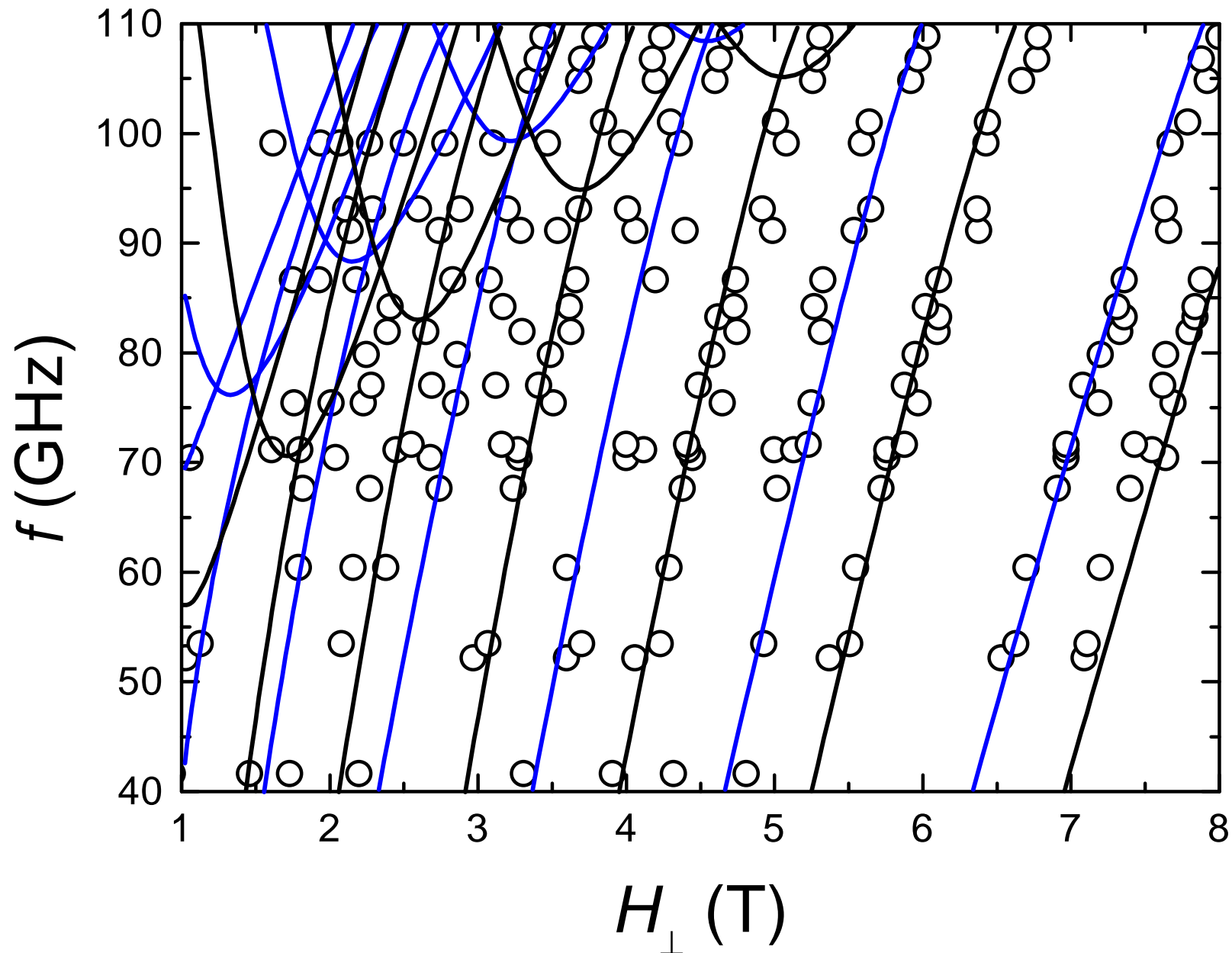


Figure 4: Amigo et al.